Single-electron computing: Quantum dot logic gates

S. N. Molotkov and S. S. Nazin

Institute of Solid State Physics of the Russian Academy of Sciences, 142432 Chernogolovka, Moscow Region, Russia

(Submitted 27 March 1996)
Zh. Éksp. Teor. Fiz. **110**, 1439–1452 (October 1996)

The possibility of realizing simple single-electron logic gates (where information is stored in spins of individual electrons) by means of arrays of tunnel-coupled quantum dots with strong intradot Coulomb interaction is considered. The exact diagonalization technique for the spin-1/2 Heisenberg model is used to analyze quantum dot structures realizing a number of the simplest logic gates (NOT, AND, NAND, OR, NOR, NXOR, and half-adder). It is shown that for all gates considered the entire truth table can be obtained by choosing appropriate values of the local magnetic fields at the dots which are regarded as the gate inputs. © *1996 American Institute of Physics.* [S1063-7761(96)02010-0]

1. INTRODUCTION

Conventional computers perform operations on classical Boolean logic variables which accept one of the two values 0 and 1. Even in today's microelectronics, each of these variables is physically associated with a macroscopic object involving millions of electrons. However, the general trend to reduce the size of computer components and increase their speed and data storage density requires gradual introduction of new nanometer scale technologies where information is stored and processed at the level of single electrons. The simplest way to establish a one-to-one correspondence between a Boolean variable and a quantum mechanical system is to associate the bit values 0 and 1 with any two eigenstates of the system (for example, the two opposite spin polarizations of an electron trapped in a potential well). The idea of using a two-state system to represent the Boolean variable values (0 and 1) was first seriously analyzed by Feynman.[1] However, it was soon realized[2] that these quantum bits ("qubits") provide much wider opportunities for information processes. Since then, there has been active research in both general problems of quantum computation and the practical design of simple quantum gates.[3,4] The point is that being a quantum system, the qubit can be found in any superposition of the two states forming the basis of the two-dimensional system space. Therefore, in a system of qubits it is possible to achieve the interference of states corresponding to different parallel computation paths. In this way it is possible to develop extremely efficient algorithms for quantum computations which are exponentially faster than any available conventional algorithms.[3,4]

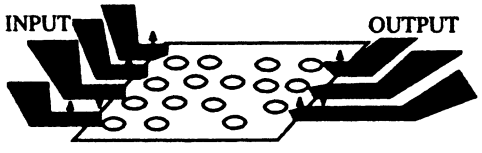

FIG. 1. Array of quantum dots on a solid surface.

However, in the present paper we shall restrict our attention to the conceptually much simpler case of single-electron spin gates first proposed by Bandyopadhyay *et al.*[15] which employ classical Boolean logic. In that approach the computer is thought of as consisting of a set of coupled spin gates, each of which is a system of interacting spins associated with a number of sites spatially configured to realize a particular logical function. In such a gate (and a computer as a whole) the stored information is determined by the spin configuration of the system ground state, i.e., a set of quantum-mechanical ground state average values of each spin $\langle \hat{S}_i \rangle$, such that $\langle \hat{S}_i \rangle < -S_t (\langle \hat{S}_i \rangle > S_t)$, where $S_t > 0$ is a certain threshold value and corresponds to logical zero (unit). Thus, here the states of a quantum system are mapped onto the Boolean variables in a less restrictive way than for reversible quantum gates, where the Boolean variables are associated with certain pure quantum states. Interaction between the gates is realized through the quantum coupling between the neighboring spins. Computing is performed by the appropriate action of an external agent (e.g., local magnetic fields) on the system input sites, which changes the system Hamiltonian so that the new ground state (its spin configuration) can represent the result of a desired computational operation. Although these gates are not *bona fide* reversible quantum gates, their analysis has much in common with the problems arising in truly quantum computing.

The spin gates we are going to consider are assumed to consist of a number of tunnel-coupled quantum dots (potential wells for electrons) fabricated on a solid surface. The following conditions are believed to be necessary to allow the realization of standard logical functions.

1. Antiferromagnetic interaction between the electrons in adjacent dots (more rigorously, antiferromagnetic correla-

TABLE I. Invertor (NOT gate) truth table.

A	Y
0	1
1	0

 1063-7761/96/100794-09$10.00

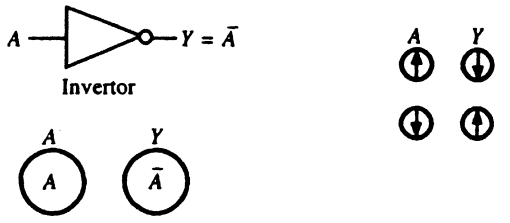

FIG. 2. Invertor (NOT gate) realized by a pair of tunnel-coupled quantum dots.

TABLE II. Truth table of the NOT-AND gate.

A	B	Y
1	1	0
0	1	1
1	0	1
0	0	1

tions between the adjacent electrons in the ground state). This condition can be satisfied if there is a strong intradot electron-electron Coulomb interaction. The tunnel coupling among the dots serves as quantum wires. Information is stored in the direction of electron spins.

2. Each dot has a single size-quantized level.

3. On the average, there is one electron per dot.

2. POSSIBLE REALIZATION BASED ON QUANTUM DOTS

The computer architecture can be described in the following way. An array of quantum dots configured to perform a particular logical function is fabricated on a solid surface (Fig. 1). Positioned at the edge of the array are probes similar to those used in spin-polarized STM. Some of these probes serve as inputs and the rest as outputs. The magnetization direction in the probes can be controlled by applying a magnetic field to their far ends (e.g., by induction coils). In that case the probes actually serve as magnetoguides. It is assumed that when information is written to the inputs, there is no current between the probes and corresponding dots, i.e., the applied voltage is zero. The electron spins at the input dots are aligned by the local magnetic fields at the probe tip. The total number of electrons in the array of quantum dots can be controlled by adjusting the substrate voltage. After the system relaxes to its new ground state, corresponding to the applied local fields, the result of the computations is read off the output dots by applying appropriate voltage between the output dots and magnetic probes, exploiting the fact that the tunneling current depends on the mutual orientation of the dot and probe tip magnetizations. The tunnel current spin-dependent component is proportional to the scalar product of the dot and probe tip magnetizations:[19,20] $I_t \propto (\mathbf{h}_{dot}\mathbf{h}_{iot})$.

Although rather speculative, the above scheme is in no way unrealistic, since all the necessary ingredients have already been separately realized experimentally.

1. An array of several thousands of ~10 Å metal clusters has been produced on a solid surface by blowing off the atoms from an STM tip.[21] Fabrication of quantum dots with a single size-quantized level will require a search for an appropriate material.

2. The tunnel current has been experimentally shown to be sensitive to the spin of single magnetic atoms at a solid surface[22,23] (~6 Å lateral resolution was achieved). Moreover, it is even possible to observe the precession of a single electron spin at the surface[24] and the electron spin resonance.[24–29]

3. Recently, an operational prototype of an integrated 100 μm size tunneling microscope fabricated on a single chip by means of microelectronics technology was demonstrated[30] (Hitachi Advanced Research Laboratory), which is an important advance in the way of solving the problem of creating a system of several STM probes separated by a controllable distance at the nanometer scale (which is impossible in conventional STM design).

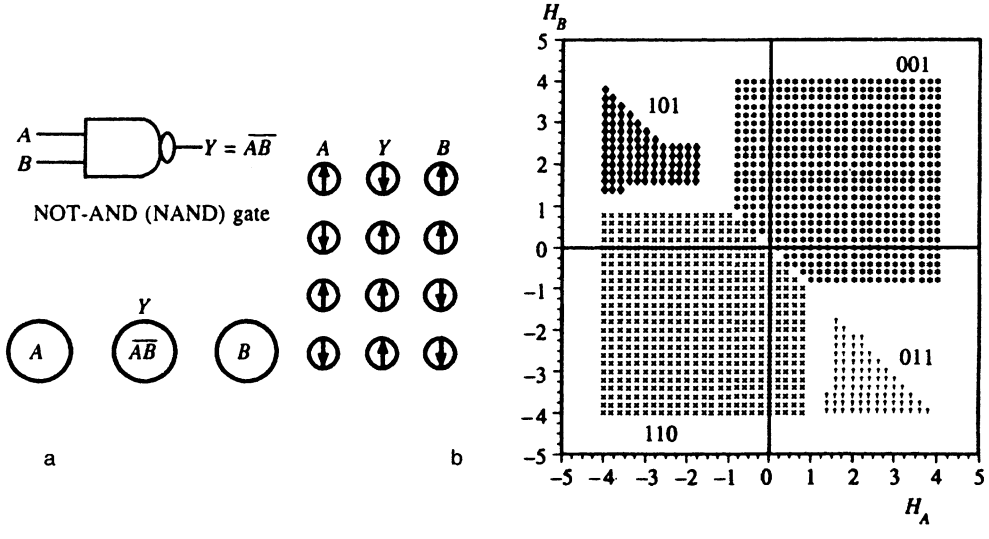

FIG. 3. Quantum dot realization (a) and physical truth table (b) of the NOT-AND gate. Domains are labeled by the corresponding lines in the truth table.

TABLE III. Truth table of the AND gate.

A	B	Y
1	1	1
0	1	0
1	0	0
0	0	0

Clearly, combining the above achievements in a single device will require much further efforts; however, these advances unambiguously indicate that the single-electron spin gates are gradually shifting to the plane of practical reality.

3. MODEL FOR THE SPIN GATES

If the intradot Coulomb repulsion is sufficiently strong, the Hubbard model at half-filling reduces to the Heisenberg model, to which we restrict our further analysis in the present paper since this simplification allows a drastic reduction of the size of matrices one has to deal with in the exact diagonalization approach. We shall consider the Hamiltonian

$$\hat{H}=J\sum_{\langle ij\rangle}\hat{\sigma}_{zi}\hat{\sigma}_{zj}+J\sum_{\langle ij\rangle}(\hat{\sigma}_{xi}\hat{\sigma}_{xj}+\hat{\sigma}_{yi}\hat{\sigma}_{yj})=J\sum_{\langle ij\rangle}\hat{\sigma}_{zi}\hat{\sigma}_{zj}$$
$$+2J\sum_{\langle ij\rangle}(\hat{\sigma}_{+i}\hat{\sigma}_{-j}+\hat{\sigma}_{-i}\hat{\sigma}_{+j}). \quad (1)$$

where $\hat{\sigma}_{z,x,yi}$ are the Pauli matrices describing the electron at site i (it is more convenient to use $\hat{\sigma}_{z,x,yi}$ instead of the spin-1/2 operators $\hat{s}_{z,x,yi}$). We shall assume that the exchange interaction favors the antiferromagnetic ordering ($J>0$).

The system is controlled by external local magnetic fields (for simplicity assumed to be parallel to the z-axis) applied to the input dots. The Hamiltonian describing the interaction with these fields is then

$$\hat{H}_{int}=\sum_{\langle\text{input}\rangle}\hat{\sigma}_{zi}h_{zi}^{\text{input}}. \quad (2)$$

Our goal is to find the physical truth tables, i.e., the range of control signals (local magnetic fields at the input dots) corresponding to the realization by the system ground state of the truth table of the logical function which should be implemented by a particular gate.

Invertor (NOT gate)

The simplest logic gate is the invertor whose truth table is given by Table I and physical implementation is shown in Fig. 2.

The operation of this gate can be completely treated analytically. Ideally, one wishes to have the state $|\downarrow\rangle$ at the output if the state $|\uparrow\rangle$ is created at the input. The exchange interaction transmits the inverted state from the input to the output. However, the pure $|\uparrow\rangle$ and $|\downarrow\rangle$ states cannot be realized at the input and output dots in any ground state since the interaction inevitably admixes other states. Therefore, the spin configuration shown in Fig. 2 (as well as for other gates) should be understood as a milder requirement on the quantum-mechanical averages $\langle\hat{\sigma}_A\rangle$ and $\langle\hat{\sigma}_B\rangle$ rather than as pure states $|\uparrow\rangle_A|\downarrow\rangle_B$ and vice versa.

In the basis of states $|\sigma_A\sigma_B\rangle$ the eigenvalue problem for the Hamiltonian (1) is written as

$$H=\begin{pmatrix}-\varepsilon+h_A+J & 0 & 0 & \\ 0 & -\varepsilon+h_A-J & 2J & 0 \\ 0 & 2J & -\varepsilon-h_A-J & 0 \\ 0 & 0 & 0 & -\varepsilon-h_A+J\end{pmatrix}. \quad (3)$$

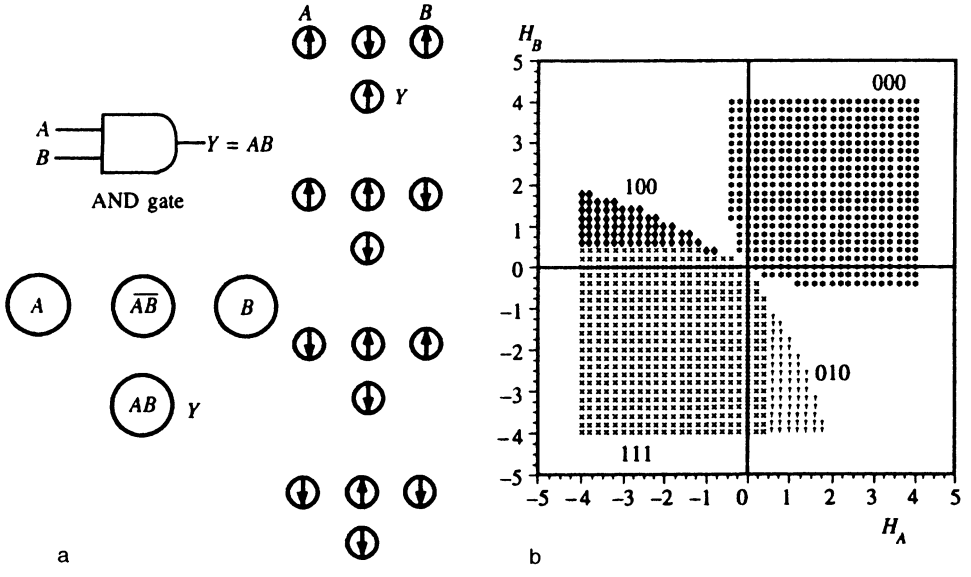

FIG. 4. Quantum dot realization (a) and physical truth table (b) of the AND gate.

TABLE IV. Truth table of the OR gate.

A	B	Y
1	1	1
1	0	1
0	1	1
0	0	0

TABLE V. Truth table of the NOR gate.

A	B	Y
1	1	0
1	0	0
0	1	0
0	0	1

The eigenenergies are: $\varepsilon_3 = -h_A + J$, $\varepsilon_3 = h_A + J$ (eigenfunctions $|\uparrow\uparrow\rangle$ and $|\downarrow\downarrow\rangle$), $\varepsilon_{1,2} = -J \pm \sqrt{h_A^2 + 4J^2}$. At zero input signal $h_A = 0$, the ground state energy is $\varepsilon_1 = -3J$ (remember that $J>0$) with the corresponding eigenvector $|\Psi_1\rangle = (|\uparrow\downarrow\rangle - |\downarrow\uparrow\rangle)/\sqrt{2}$. The eigenvector associated with the level $\varepsilon_1 = -J$ is $|\Psi_2\rangle = (|\uparrow\downarrow\rangle + |\downarrow\uparrow\rangle)/\sqrt{2}$. For zero magnetic field at the input dot the system ground state is a mixed state (a state which cannot be factored) in which neither input nor output bits have a definite value. When a control signal is fed to the input, the ground state turns into

$$|\Psi_{gr}\rangle = u|\uparrow\downarrow\rangle + v|\downarrow\uparrow\rangle. \tag{4}$$

where

$$\begin{Bmatrix} u^2 \\ v^2 \end{Bmatrix} = \frac{1}{2}\left(1 \pm \frac{h_A}{\sqrt{h_A^2 + 4J^2}}\right).$$

The quantum-mechanical averages of the input and output dot spins become

$$\langle S_A\rangle = \langle\Psi_{gr}|\hat{\sigma}_A|\Psi_{gr}\rangle = u^2 - v^2 = \frac{h_A}{\sqrt{h_A^2 + 4J^2}}, \tag{5}$$

$$\langle S_Y\rangle = \langle\Psi_{gr}|\hat{\sigma}_Y|\Psi_{gr}\rangle = v^2 - u^2 = -\frac{h_A}{\sqrt{h_A^2 + 4J^2}}. \tag{6}$$

Thus, nonzero average spins arise only to the extent that the external magnetic field at the input dot is different from zero. The equality $\langle\hat{\sigma}_A\rangle = -\langle\hat{\sigma}_Y\rangle$ is always satisfied, just as required by the truth table. The physical truth table for the invertor (the range of magnetic fields at the input dot where the spin configurations required by Table I are realized) consists of two parts. In the first one ($h_A > 0$)the first row of Table I is reproduced, and in the second one ($h_A < 0$) the second row is realized. Formally both these regimes can be achieved at arbitrarily low magnetic fields (although with equally small average spins).

The above example demonstrates how the interaction between the adjacent dots can serve as a "quantum lead" and transmit the signal from the input to the output dot.

NOT-AND (NAND) gate

This gate has two control inputs (A and B) and one output (Y). Its truth table is given by Table II and the physical realization based on quantum dots is shown in Fig. 3a.

This gate can also be analyzed analytically; in the basis $|\uparrow\uparrow\uparrow\rangle$, $|\uparrow\uparrow\downarrow\rangle$, $|\uparrow\downarrow\uparrow\rangle$, $|\downarrow\uparrow\uparrow\rangle$, $|\uparrow\downarrow\downarrow\rangle$, $|\downarrow\uparrow\downarrow\rangle$, $|\downarrow\downarrow\uparrow\rangle$, $|\downarrow\downarrow\downarrow\rangle$ its Hamiltonian can be written as

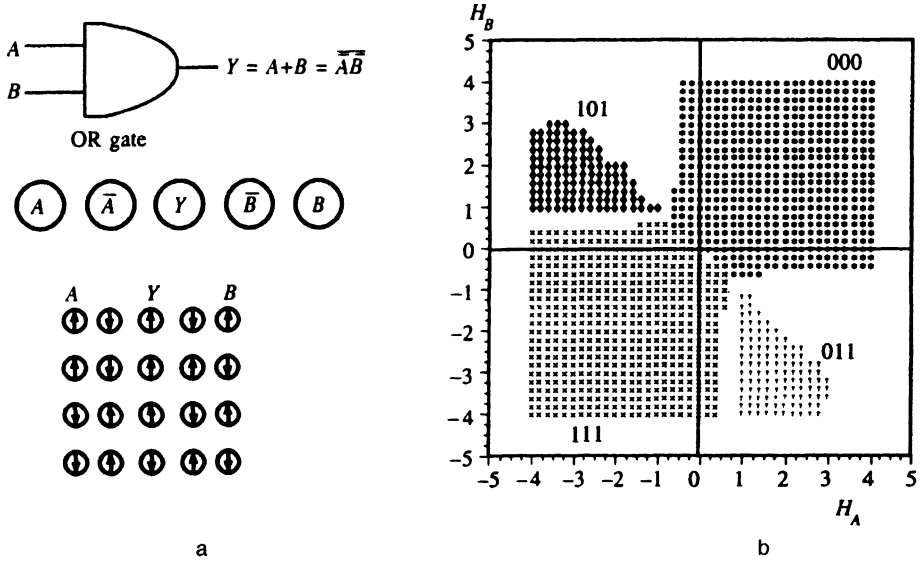

FIG. 5. Quantum dot realization (a) and physical truth table (b) of the OR gate.

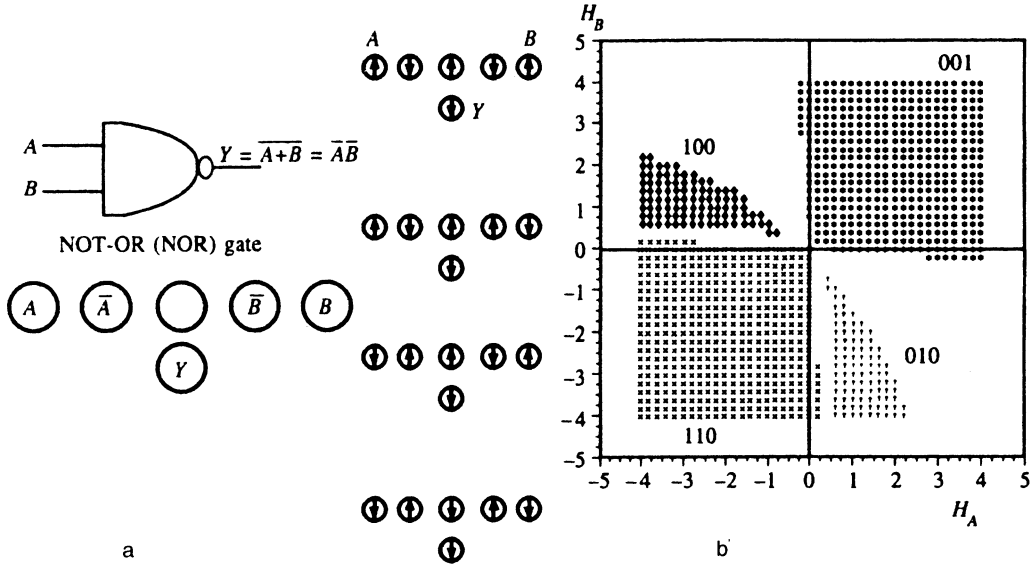

FIG. 6. Quantum dot realization (a) and physical truth table (b) of the NOR gate.

$$H=\begin{pmatrix} \varepsilon^{+}_{++} & 0 & 0 & 0 & 0 & 0 & 0 & 0 \\ 0 & \varepsilon_{--} & 2J & 0 & 0 & 0 & 0 & 0 \\ 0 & 2J & \varepsilon^{-}_{++} & 2J & 0 & 0 & 0 & 0 \\ 0 & 0 & 2J & \varepsilon_{-+} & 0 & 0 & 0 & 0 \\ 0 & 0 & 0 & 0 & \varepsilon_{-+} & 2J & 0 & 0 \\ 0 & 0 & 0 & 0 & 2J & \varepsilon^{-}_{--} & 2J & 0 \\ 0 & 0 & 0 & 0 & 0 & 2J & \varepsilon_{+-} & 0 \\ 0 & 0 & 0 & 0 & 0 & 0 & 0 & \varepsilon^{+}_{--} \end{pmatrix}, \tag{7}$$

where

$$\varepsilon_{--}=-\varepsilon+h_A+h_B, \quad \varepsilon_{+-}=-\varepsilon+h_A-h_B,$$

$$\varepsilon_{-+}=-\varepsilon-h_A+h_B, \quad \varepsilon_{--}=-\varepsilon-h_A-h_B,$$

$$\varepsilon^{\pm}_{\alpha,\beta}=\varepsilon_{\alpha,\beta}\pm 2J, \quad \alpha,\beta=\{+,-\}.$$

In zero magnetic field the eigenenergies and corresponding eigenvectors are:

$$|\Psi_{gr}\rangle=\frac{1}{\sqrt{6}}|\uparrow\uparrow\downarrow\rangle-\sqrt{\frac{2}{3}}|\uparrow\downarrow\uparrow\rangle+\frac{1}{\sqrt{6}}|\downarrow\uparrow\uparrow\rangle \quad \varepsilon=-4J,$$

$$|\Psi_0\rangle=\frac{1}{\sqrt{2}}(|\uparrow\uparrow\downarrow\rangle-|\downarrow\uparrow\uparrow\rangle) \quad \varepsilon=0,$$

$$|\Psi^1_{2J}\rangle=|=|\uparrow\uparrow\uparrow\rangle, \quad |\Psi^2_{2J}\rangle=\frac{1}{\sqrt{3}}(|\uparrow\uparrow\downarrow\rangle+|\uparrow\downarrow\uparrow\rangle$$

$$+|\downarrow\uparrow\uparrow\rangle, \quad \varepsilon=2J,$$

and those obtained from the above by reversing the spins at all sites (Kramers degeneracy). Note that in zero magnetic field all the states (including the ground state) are doubly degenerate.

It is not obvious whether there exist ranges of the control parameters h_A and h_B implementing the entire truth table of the gate. Formally, the problem can be formulated as follows: is it possible to modify the ground state spin averages at the relevant dots in the required way by adjusting the external magnetic fields only?

Results of numerical analysis of the physical truth table are presented in Fig. 3b. (Here and below, unless stated otherwise, we have chosen the spin threshold $S_t=0.1$, i.e., the electron spin at a particular dot is assumed to point upwards (downwards) if the condition $\langle\sigma_z\rangle > 0.1(\langle\sigma_z\rangle < -0.1)$is satisfied). Each row in the truth table (Table II) corresponds to a domain in Fig. 3b. The first row is easily realizable: if the magnetic fields at dots A and B align electron spins upwards, the antiferromagnetic exchange maintains the output spin in the downwards position, and a similar situation occurs for the last row. These spin configurations are "natural" for the antiferromagnetic interdot coupling, and the input magnetic fields only lift the degeneracy between these two states. It is less obvious that the second and third rows in Table II can also be realized. Although the corresponding spin configurations are not favored by the antiferromagnetic coupling, they still can be realized by applying sufficiently high input mag-

TABLE VI. Truth table of the NXOR gate.

A	B	Y
0	0	1
0	1	0
1	0	0
1	1	1

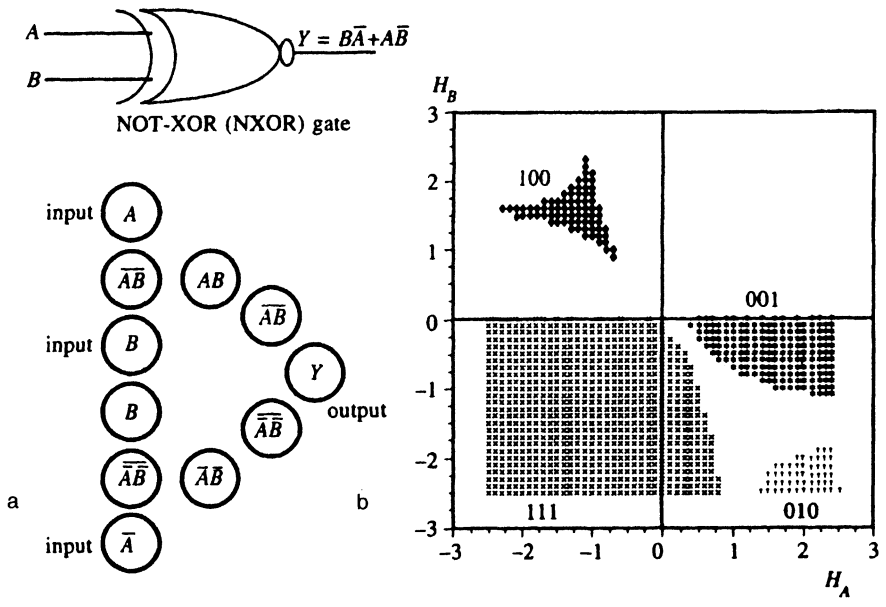

FIG. 7. Quantum dot realization (a) and physical truth table (b) of the NXOR gate (S_t=0.05).

-netic fields compensating for large exchange energy due to parallel spins at adjacent dots.

AND gate

The next in complexity is the AND gate which can be obtained from the preceding gate adding the invertor to its output ($\bar{Y}$). The logical truth table and quantum dot realization are presented in Table III and Fig. 4a, respectively. The total number of states here, $2^4 = 16$, is rather large and the problem can only be solved numerically.

The physical truth table obtained by the exact diagonalization technique and shown in Fig. 4b reveals that by adjusting the input magnetic fields it is possible to realize the entire truth table. As with the NAND gate, some configurations can only be realized at finite magnetic fields (on the order of the exchange coupling, if measured in energy units) while the "natural" configurations are realized at arbitrarily low magnetic fields (for spin threshold S_t=0).

OR gate

The OR logic gate has two inputs (A and B) and one output (Y); its truth table is given by Table IV, and its physical realization consisting of five quantum dots (total number of states $2^5 = 32$) is shown in Fig. 5a.

Note that the states of inputs A and B in this gate are "transferred" to the output Y through the pieces of a "quantum wire" built of the intermediate quantum dots. Just as in previous cases, the entire truth table can be realized for sufficiently high input magnetic fields.

NOT-OR (NOR) gate

This gate is obtained from the preceding one (OR gate) by inverting the output signal achieved by adding one more dot. The logical and physical truth tables are presented in Table V and Fig. 6a, respectively. It is seen from Fig. 6a that all the required spin configurations can be realized for arbitrary small input magnetic fields.

NOT-XOR (NXOR) gate and half-adder

A possible realization of the NOT-excluding-OR gate (NXOR gate, see Table VI and Fig. 7a) involving 11 dots (total number of states is 2048) was proposed in Ref. 15.

Note that the realization of the NXOR gate requires three rather than two physical inputs: one has to introduce an additional input representing the inverted A signal ($\bar{A}$, see Fig. 7a). In modelling this gate, it was assumed that equal in magnitude and opposite in direction magnetic fields h_A and $-h_A$ were applied to the inputs A and $\bar{A}$, respectively, and the field h_B was applied to input B. To obtain the XOR gate, one should simply add one more dot next to the output so that the resulting combination of the NXOR gate and an invertor produce the required XOR gate. However, this modification would result in too large matrices which could not be diagonalized in reasonable time on our computers.

The only difference between the half-adder and the XOR gate is that the former has one more output (C) representing the carry bit. The output Y corresponds to the sum (Σ) of two bits at the inputs A and B. Since we cannot consider the true half-adder obtained from the 12-dot XOR gate, we analyze the gate which we for obvious reasons rather arbitrarily call

TABLE VII. NOT-half-adder truth table.

A	B	Σ	C
0	0	1	0
0	1	0	0
1	0	0	0
1	1	1	1

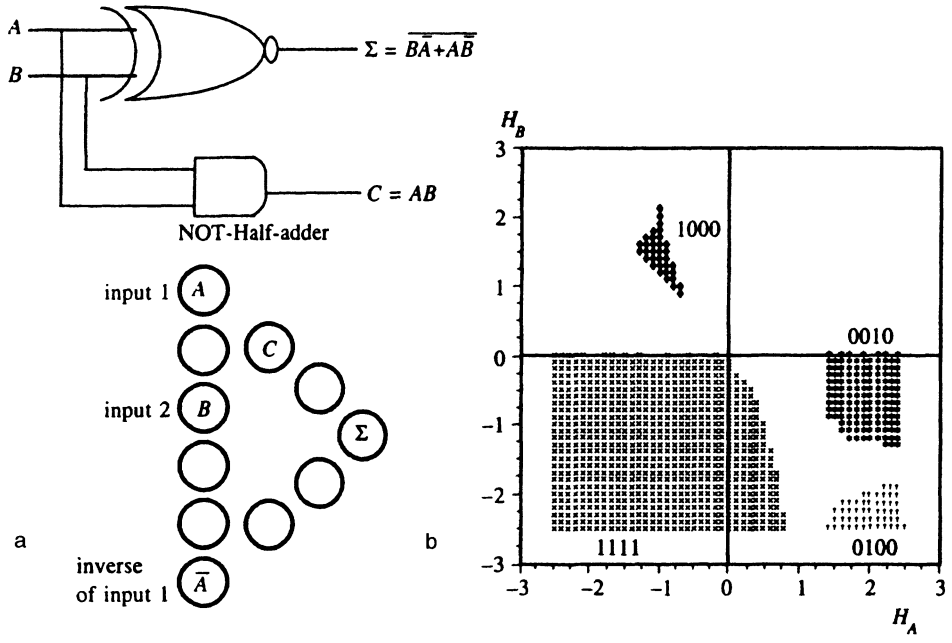

FIG. 8. Quantum dot realization (11 dots) (a) and physical truth table (b) of the NOT-half-adder (S_t=0.05).

"NOT-half-adder." The truth table of the NOT-half-adder is given by Table VII, and its physical realization, identical to that of the XOR gate, is shown in Fig. 8a. Here again the total number of states is 2048.

The physical truth table of the NOT-half-adder is obtained from that of the XOR gate by imposing an additional constraint on the average spin value at the C dot (carry bit); therefore, it is actually a proper subset of the XOR physical truth table. The problem is whether or not all the domains of the XOR physical truth table survive after the appropriate restriction on the electron spin at dot C is imposed. Figure 8b reveals that the answer is affirmative. Although two of the domains are seen to substantially shrink after this procedure, they are all retained in reasonable magnetic fields. Note that the threshold spin S_t for both Figs. 7b and 8b was chosen to be 0.05; the reason is that for S_t=0.1 the domain corresponding to the 0100 spin configuration (second row in Table II) completely vanishes. In addition, a tiny island at low magnetic fields ($H_A<0$, $H_B>0$ in the third quadrant) where the 010 and 0100 spin configurations are realized also vanishes; other domains are not so severely affected by this change. Therefore, the logic truth table cannot be fully realized with $S_t \geqslant 0.1$.

Note that the above NXOR realization is not the only possible one. For example, it is even possible to construct the XOR gate (Table VIII, Fig. 9) and the true half-adder with only 9 dots (Table IX, Fig. 10) at the expense of introducing additional input for the inverted B signal.

The physical truth tables shown in Figs. 7b and 8b exhibit one striking feature. The point is that the domains corresponding to the 001 (Fig. 7b) and 0010 (Fig. 8b) spin configurations are located in the domain where $H_A>0$, $H_B<0$, rather than in the intuitively expected domain $H_A>0$, $H_B>0$. This circumstance can present an obstacle on the integration of separate gates into a single network, since the input spin configuration $\langle S_A \rangle > 0$, $\langle S_B \rangle > 0$ (which should itself be taken as the output of the preceding stages of a particular operation in the quantum dot array and transferred to the inputs of the NXOR gate through the chains of quantum dots) is expected to be represented by input signals with $H_A>0$, $H_B>0$. Perhaps the most suitable for the network integration would be the situation where the domains in the physical truth table corresponding to different rows in the logic truth table are characterized by magnetic fields H_0 of approximately the same magnitude common to all gates [i.e., are located in the neighborhood of points (H_0,H_0), $(H_0, -H_0)$, $(-H_0, H_0)$, and $(-H_0, -H_0)$]. At present, we have some preliminary results for the simplest gates indicating that this goal can be achieved if one considers the anisotropic Heisenberg model ($J_x = J_y < J_z$) and introduces additional constant local magnetic fields at appropriate dots in the gate.

TABLE VIII. Truth table of the XOR gate.

A	B	Y
0	0	0
0	1	1
1	0	1
1	1	0

TABLE IX. Half-adder truth table.

A	B	Σ	C
0	0	0	0
0	1	1	0
1	0	1	0
1	1	0	1

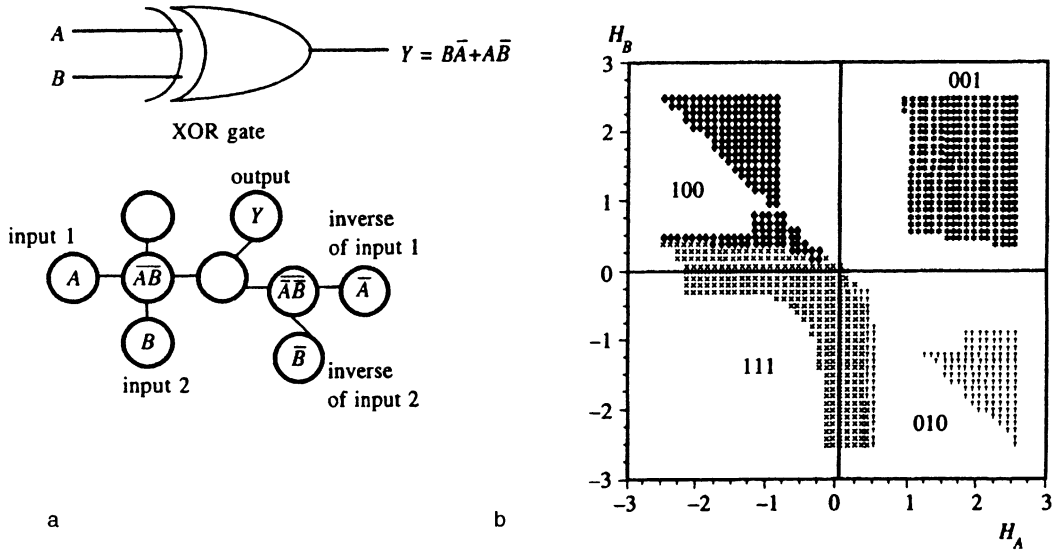

FIG. 9. Quantum dot realization (9 dots) (a) and physical truth table (b) of the XOR gate.

4. CONCLUSION

We have studied the possibility of achieving ground state computing with quantum coupled architecture in the structures of tunnel-coupled quantum dots on a solid surface. Because of computer resource limitations, we were only able to consider gates containing no more than 11 quantum dots. The gates investigated include NOT, NAND, AND, OR, NOR, NXOR gates and half-adders. The results obtained reveal that for all these gates the input local magnetic fields can be chosen so as to realize the entire truth tables. Strictly speaking, in the quantum coupled architecture the entire computer should be described by a single wave function corresponding to the ground state of the system as a whole. Therefore, it is important to find out whether the spin correlations can be maintained throughout large arrays of quantum dots. The present study reveals that the interdot exchange interaction is sufficiently strong to ensure the required "magnetic orders" (ground state spin configurations) even in the largest considered gates, although for the half-adder realized on 11 dots one of the domains in the physical truth table is rather small, which seems to be related to the fact that for this gate each line in the logical truth table imposes restrictions on the spin orientations at four quantum dots rather than three as it was the case for all other nontrivial gates. Hence, it would be very interesting to consider a quantum dot realization of the adder gate which should have three inputs (the bits A and B to be added, and the carry input C_{in}) and two outputs (the result of addition of A and B module 2 and the carry output C_{out}). Unfortunately, analysis of such a scheme is beyond our current computer resources.

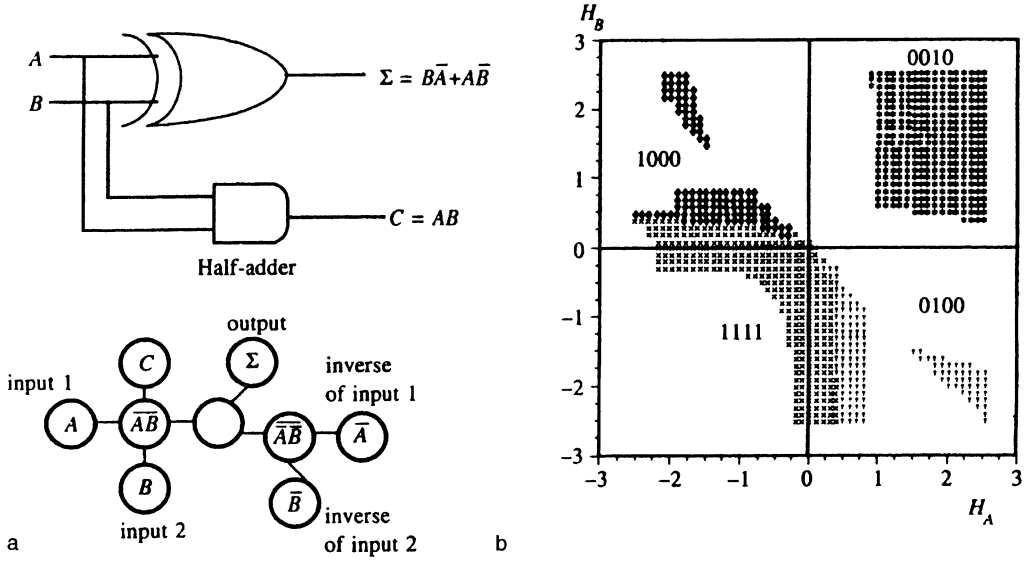

FIG. 10. Quantum dot realization (9 dots) (a) and physical truth table (b) of the half-adder without inversion of output.

This work was supported by the Russian Fund for Fundamental Research (Grant No. 96-02-18918) and by Grant No. 110/57/1–3 from the State National Technology Program "Advanced Technologies in Micro- and Nanoelectronics."

[1] R. Feynman, Int. J. Theor. Phys. **21**, 467 (1982); Foundations of Phys. **16**, 507 (1986).
[2] D. Deutsch, Proc. Roy. Soc. A **400**, 97 (1985); D. Deutsch, Proc. Roy. Soc. A **425**, 73 (1989); D. Deutsch and R. Jozsa, Proc. Roy. Soc. A **439**, 553 (1992).
[3] P. Shor, in *Proc. of the 35th Annual Symposium on the Foundation of Computer Science*, IEEE Computer Society, Los Alamitos, CA (1994), p. 124.
[4] C. H. Bennet, Physics Today **48**, 24 (1995).
[5] W. K. Wootters and W. H. Zurek, Nature **299**, 802 (1982).
[6] A. Barenco, D. Deutsch, and A. Ekert, Phys. Rev. Lett. **74**, 4083 (1995).
[7] S. Lloyd, Phys. Rev. Lett. **75**, 346 (1995).
[8] S. Lloyd, Science **261**, 1569 (1993).
[9] T. Pellizzari, S. A. Gardiner, J. I. Cirac, and P. Zoller, Phys. Rev. Lett. **75**, 3788 (1995).
[10] J. I. Cirac and P. Zoller, Phys. Rev. Lett. **74**, 4091 (1995).
[11] T. Stealor and H. Weinfurter, Phys. Rev. Lett. **74**, 4087 (1995).
[12] Q. A. Turchette, C. J. Hood, W. Lange *et al.*, Phys. Rev. Lett. **75**, 4710 (1995).
[13] C. Monroe, D. M. Meekhof, B. E. King *et al.*, Phys. Rev. Lett. **75**, 4714 (1995).
[14] D. P. DiVincenzo, Phys. Rev. A **51**, 1015 (1995).
[15] S. Bandyopadhyay, B. Das, and A. E. Miller, Nanotechnology **5**, 113 (1994).
[16] S. Bandyopadhyay, V. P. Roychowdhury, and X. Wang, Phys. Low-Dim. Struct. **8/9**, 28 (1995).
[17] S. Bandyopadhyay and V. P. Roychowdhury, *Computational Paradigm in Nanoelectronics: Single-Electron Logic and Neuromorphic Networks*, (invited paper presented at SSDM'95, Osaka, Japan, August 1995).
[18] S. N. Molotkov and S. S. Nazin, JETP Lett. **62**, 256 (1995).
[19] S. N. Molotkov, JETP Lett. **55**, 173 (1992).
[20] S. N. Molotkov, Surface Science **261**, 7 (1992).
[21] H. J. Mamin, P. H. Guethner, and D. Rugar, Phys. Rev. Lett. **65**, 2418 (1990).
[22] R. Wiesendanger, H.-J. Güntherodt, R. J. Cambino, and R. Ruf, Phys. Rev. Lett. **65**, 583 (1990).
[23] I. V. Shvets, R. Wiesendanger, D. Bürgler *et al.*, J. Appl. Phys. **71**, 5489 (1992).
[24] Y. Manassen, R. J. Hamers, J. E. Demuth, and A. J. Castellano, Jr., Phys. Rev. Lett. **62**, 2513 (1989).
[25] A. W. McKinnon and M. E. Weland, in *Abstracts STM'91, International Conference on Scanning Tunneling Microscopy*, Interlaken (1991), p. 51.
[26] S. N. Molotkov, Surface Science **264**, 235 (1992).
[27] S. N. Molotkov, Surface Science **302**, 235 (1994).
[28] S. N. Molotkov and S. S. Nazin, Surface Science **304**, 109 (1994).
[29] S. N. Molotkov and S. S. Nazin, Phys. Low-Dim. Struct. **9**, 21 (1994).
[30] M. I. Lutwwyche and Y. Wada, J. Vac. Sci. Technol. B **13**, 2819 (1995).

Published in English in the orignal Russian journal. Reproduced here with stylistic changes by the Translation Editor.